

INVESTIGATION THE EFFECT OF POROSITY ON CORROSION RESISTANCE AND HARDNESS OF WC-Co COATINGS ON METAL SUBSTRATES

O.P. Oladijo ^{a*}, B.A. Obadele ^c, A.M. Venter ^{d,e}, and L.A. Cornish ^{b,d}

^a Department of Chemical, Materials and Metallurgical Engineering, Botswana International University of Science and Technology, Palapye, Botswana

^b School of Chemical and Metallurgical Engineering, University of the Witwatersrand,

^c Department of Chemical Engineering, University of Johannesburg, Doornfontein Campus, Johannesburg

^d DST/NRF Centre of Excellence in Strong Materials, hosted by the University of the Witwatersrand

^e Research & Development Division, NECSA Limited, Pretoria

ABSTRACT

Porosity is an important coating feature which strongly influences coating properties. Porosity creates poor coating cohesion and allows for higher corrosion rate and wear, and is generally associated with a higher number of unmelted or solidified particle that become trapped in the coating [1]. This investigation was conducted to investigate the effect of porosity on the hardness and corrosion resistance of WC-17Co coating on metal substrates. Coating of about 200 μ m were successfully deposited by HVOF techniques onto four metal substrates, namely brass, 304L stainless steel, super-invar and aluminium. The corrosion behaviour was examined in chloride medium using direct current (DC) polarization test. The Vickers hardness was undertaken at loads of 5 kg for 10 s. The microstructures of the coatings were studied before and after the corrosion tests by scanning electron microscopy with EDX. The results indicated a strong correlation between porosity and corrosion rate, as well as hardness of the WC-17Co coatings.

Keywords: Porosity, HVOF, Thermal spray, WC-Co coating, Metal substrate, NaCl

1. Introduction

Corrosion of metallic materials remains a technological and major economic challenge. The lifespan of products containing metallic component is mostly limited by the corrosion of the metallic parts [Marcus *et al.* 1998]. The gross domestic product of the cost of corrosion of metals and alloy has been estimated to be 25%, and one estimated that 25% of this cost could be saved with proper better control measure [Marcus *et al.* 1998]. It is also thought that the combine action of corrosion and wear often results in a significant increase in material loss that is much higher than the sum of the individual contribution of wear and corrosion [Basak *et al.* 2006]. Therefore thermal spraying techniques have been considered as one the method to prevent or combat corrosion and wear resistance of metallic material by many researchers. One of such materials, which attracted interest from many researchers, is tungsten carbide [Vamsi Krishna *et al* 2002].

Electroplated hard chrome coating has been using for the corrosion protection of structural aircraft component, such as landing gear due to its combined good hardness, wear resistance and adequate corrosion resistance [Ward *et al.* 2011]. However, the effect of calcinogenic caused hexavalent chromium salts associated with the plating has prompted the users or industries to look for an alternative as reported by [Ward *et al.*]. One of the considerable interest is also the used of thermal spray WC- based coating.

The corrosion behaviours of WC-Co and WC-Co-Cr sprayed coating in Na₂SO₄ an aqueous solution was studied by Takeda *et al* 2001. The corrosion resistance of WC-Co-Cr coating was found to be higher than that of WC-Co coating. This was attributed to the formed passive film containing chromium. The structural investigations and properties evaluation of WC-CoCr and WC-Cr-Ni coating was investigated by Dragos *et al.* [2012]. They found that both coatings are dense (porosity about 1%), compact and without defects as cracks. The corrosion resistance of the WC-CoCr coating in a 1M NaCl was higher than that of the WC Cr Ni coating due to the chemical composition differences of the metallic matrix.

The high velocity WC-Co coatings thermally sprayed by High Velocity Oxy-fuel Flame (HVOF) are widely used in many industries due to high melting point, wear resistance, good thermal shock resistance against oxidation [Vamsi Krishna *et al* 2002, Oladijo *et al.* 2012]. High velocity oxy-fuel techniques spraying process has been considered as one of the best deposition techniques for obtaining excellent quality coatings of low porosity, high density with better bond strength [Dragos *et al.* 2012]. In addition, thermal sprayed coatings onto the

surface of engineering component that operate in both aggressive and chloride medium can prevent their surface degradation by corrosion, erosion or combined erosion-corrosion. It is thought that the ability of these thermal sprayed coatings to protect base metal against aggressive environment is given by their composition, morphology and structure, whilst microstructural features which played an important role in coating corrosion resistance includes high density, low porosity, small grain size, absence of crack [Dragos *et al* 2012, Wang *et al* 1994]. Therefore the studied of porosity is crucial for better understanding of the material properties and its corrosion resistance.

Porosity is an important coating feature which strongly influences the coating properties. Porosity creates poor coating cohesion and allows for higher corrosion rate and wear, and is generally associated with a higher number of unmelted or solidified particle that become trapped in the coating [Crawmer *et al* 2005]. It is thought that the thermal sprayed coatings are often porous depending on the techniques used for deposition as well as their spraying parameters. Vacadio *et al* [2000] reported that the electrochemical corrosion resistance of a metal coated by thermal spraying techniques is not limited by the intrinsic corrosion resistance of the deposit, but also by the porosity of the coating. The Corrosion behaviour of modified HVOF sprayed WC based cermet coatings on 409 ferritic stainless steel in salt spray was investigated by Ward *et al.* 2006. Their results revealed poor corrosion performance by all the three coatings. This was attributed to the high level of porosity, the presence of micro-cracks within the coating, resulting in attack of the substrate directly by the saline environment. In addition, their potentiodynamic scanning studied revealed poor corrosion performance of the coatings when compared with the stainless steel substrate. This was attributed to the poor structure and possible galvanic coupling effects between the substrate and the coating.

The authors previously reported the characterization and abrasive wear resistance of these coatings elsewhere [Oladijo 2012], as well as the correlation between the residual stress and abrasive wear resistance [Oladijo 2014]. However, little information is at present available on the corrosion response of thermally-spray WC cermet coatings particularly with a Co binder in different environments. Therefore, this investigation was conducted to investigate the effect of porosity on the hardness and corrosion resistance of HVOF sprayed WC-17Co on four different metallic substrates. The corrosion resistance was examined in NaCl medium, using electrochemical potentiodynamic scanning studies and scanning electron microscopy, equipped with electron discharge spectroscopy (SEM/EDS).

2. Experimental Procedure

A square plate 304L stainless steel, brass, super-invar and aluminium 2xxx alloy were sectioned from 10 mm thick sheet having dimension 75 mm x 25 mm. The substrate samples were grit-blasted by alumina grit to remove and surface contaminants and improve coating – substrate adhesion prior deposition of coating. A commercial spray dried and sintered WC-17Co powder with a size distribution of 15 – 45 μ m was used deposited onto the four substrate plate using commercial facilities. The spraying coating thickness was about 200 μ m. The parameters were the same on all coated samples and were: 4 in. gun barrel; 380 mm spray distance; 0.0227 m³/h fuel (kerosene) flow rate; and 56.6 m³/h oxygen flow rate, as used before [Oladijo et al. 2012, Oladijo et al. 2014].

The specimens for corrosion testing were prepared by attaching an insulated copper wire using aluminium tape to one face of the specimen and cold mounting it in an epoxy resin, except for the measurement area of 1 cm². Open circuit potential (OCP) and potentiodynamic polarization tests were employed at room temperature (22 \pm 2 $^{\circ}$ C) in 3.5 % NaCl solution. The corrosion experiments were carried out on an Autolab potentiostat/galvanostat PGSTAT30, using a three electrode corrosion cell setup with a saturated Ag/AgCl as the reference electrode and a platinum rod as the counter electrode. Polarization measurements were carried out at a scan rate of 2 mV.s⁻¹ with the potential from -0.5 V to +1.5 V. Before starting the polarization scan, the specimens were cathodically polarized at -1.0 V for 15 min, followed by open circuit potential stabilization for about 2 h. In all cases, triplicate experiments were carried out to ensure reproducibility.

Characterization of the coatings of about 200 μ m thickness is reported elsewhere [10] with the data relevant to this work listed in Table 1 for ease of reference. For microstructural analysis, cross sectional micrographs and coating surface were observed by (SEM) equipped with energy disperse analysis (EDS) before and after the corrosion test respectively, in order to evaluate the morphology and corrosion mechanism. The microhardness measurement was conducted on the cross sections of the sample using Vickers indenter at loads of 5kg for 10 seconds. The reported hardness is the average values of five measurements listed in Table 1. The porosity of the coatings was measured on the cross section by dot counting.

Table 1: Coating properties [Oladijo et al. 2012 and Oladijo et al. 2014]

Coated sample	Porosity (%)	Hardness (MPa)	WC grain size (μm)	Surface roughness (nm)
Al 2xxx alloy	0.5149 \pm 0.001	10.22 \pm 0.02	0.150 \pm 0.01	35
Brass	0.4581 \pm 0.002	10.04 \pm 0.01	0.127 \pm 0.01	32
304L SS	0.5596 \pm 0.001	9.41 \pm 0.01	0.185 \pm 0.02	10
S-Invar	0.7529 \pm 0.001	7.91 \pm 0.01	0.133 \pm 0.02	24

3. Results and discussion

3.1. Coating Microstructure

Figure 1(a) show the morphology of the feedstock powder. The images of the powder reveal a spherical morphology with EDS confirming the presence of tungsten carbide grain in a cobalt matrix.

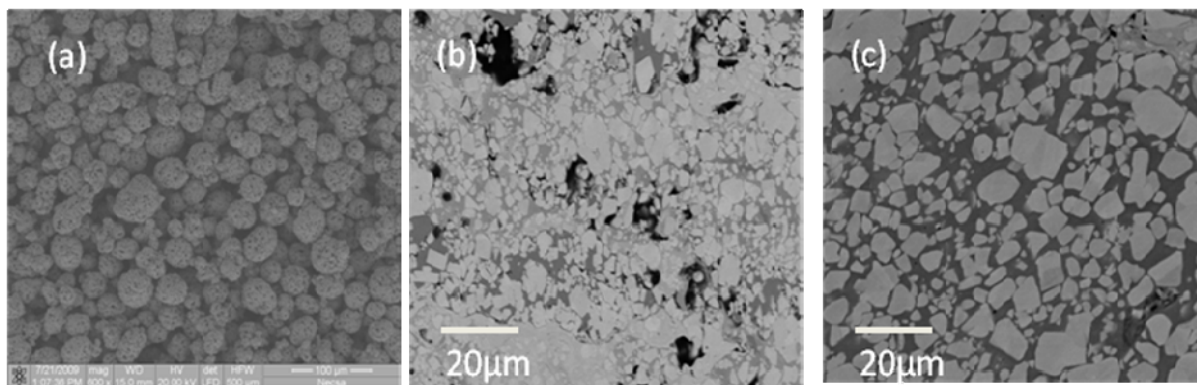


Figure 1. SEM images of the (a) WC-17Co powder, as-sprayed WC-17Co coating on (a) brass, and (b) super-invar.

The full coating characterization has been reported elsewhere [Oladijo et al. 2012 and Oladijo et al. 2014], but the representative of the coated sample cross section are presented in Figure 1(b & c). These figures shows main feature of the coatings, highlighting the differences between them. The microstructure of the as-sprayed coating on brass (Figure 1(b)) and super-invar (Figure 1(c)) had pores, microcracks, and mainly equiaxed carbide in the cobalt matrix. Also little bigger WC were found on the coating. This could be due to the accumulation of high speed molten and unmolten particles on the substrate.

3.2. Electrochemical Behavior

3.2.1. Open Circuit Potential (OCP)

Figure 2 shows the OCP of the coatings in aerated 3.5% NaCl solution. It could be observed that the open circuit potential for brass coating (-0.45 V) was nobler than that of the other coatings. It is expected that the recorded rest potential could significantly affect the corrosion behavior of the WC-Co coating layers. From the onset of potential measurement, the curve for brass coating was relatively steady throughout the measurement duration and stabilized at the highest noble values, showing the spontaneity of passive film formation. For the aluminium coating, the potential increased sharply for about 100 s, followed by a steady state and afterward a slight drop. The initial increase in potential showed the spontaneous passivation of the coating when exposed to the NaCl solution.

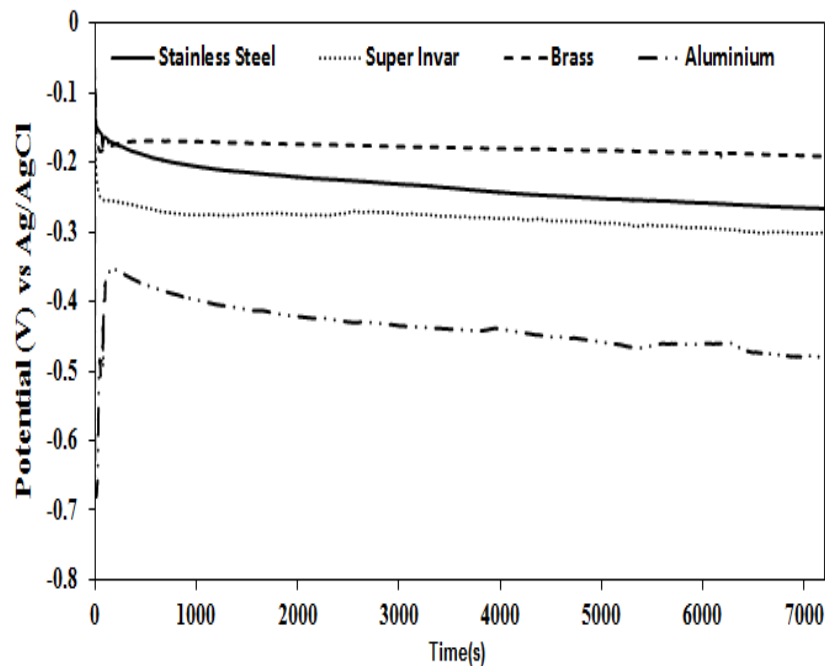


Figure 2. Open circuit potential results of the samples exposed to 3.5% NaCl.

3.2.2. Potentiodynamic Polarization Measurements

The potentiodynamic polarization curves of the coating layers in the aerated 3.5% NaCl solution at room temperature is shown in Figure 3, and the values given in Table 1. The anodic polarization curves of the coatings were quite different, with brass coating displaying

a nobler potential due to early formation of stable film. Furthermore, all the coatings displayed pseudo-passive regions in the range of -0.6 V to -1.0 V, except for stainless steel coatings which shows complete passivation. It is generally known that stainless steels passivate in NaCl solutions as a result of the presence of oxides of chromium formed on the exposed surface. This could also influence the coatings performance. On the other hand, the cathodic and anodic curves of stainless steel and super Invar are quite similar, indicating the same coating effects on the respective substrates. This might also be attributed to Ni content in both stainless steel and super invar, therefore, displaying similar polarisation curves. However, both coatings exhibited different pitting potentials, E_{pit} , with stainless steel E_{pit} fairly higher at -0.11 V, while E_{pit} for super invar is -0.16 V.

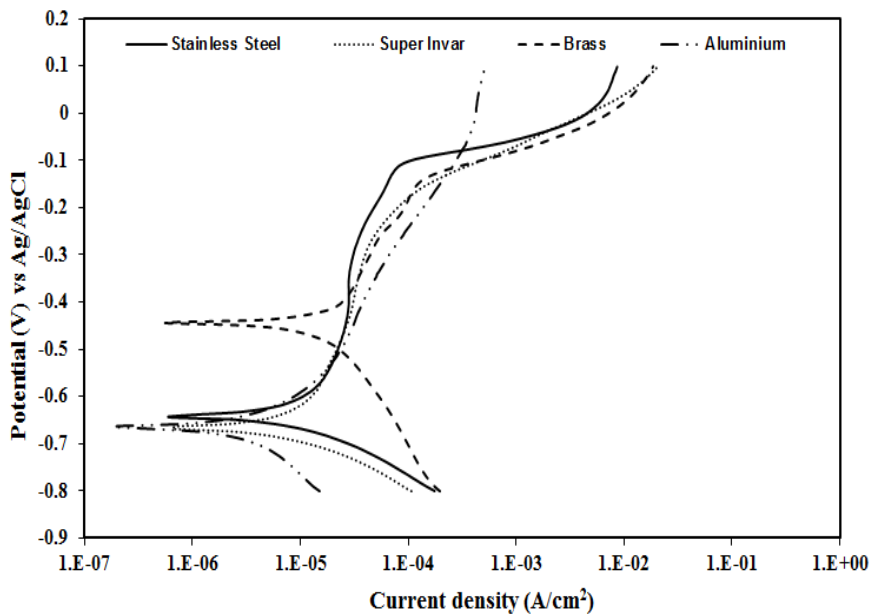


Figure 3. Potentiodynamic polarization curves of the coating layers in the aerated 3.5% NaCl solution.

Generally, the corrosion potential, E_{corr} , of the Brass coating layer was higher than that of the others due to the passive film formation. However, it exhibited the highest corrosion current density. From Table 1, corrosion current density, i_{corr} , for brass coating is $10.33 \mu\text{A}/\text{cm}^2$ while i_{corr} for stainless steel, super invar and aluminium coatings are 6.50 , 5.42 and $3.37 \mu\text{A}/\text{cm}^2$ respectively which is lower than that of brass coating. For all the coatings, the anodic current does not decrease or remain constant with increasing potential, but increases only slightly, showing pseudo-passive state.

Table 1. Corrosion data obtained after potentiodynamic polarization in 3.5% NaCl.

Coating	E_{corr}/mV	$i_{corr}/(\mu\text{A}\cdot\text{cm}^{-2})$
SS	-0.642	6.50
SI	-0.669	5.42
Brass	-0.446	10.3
Al 2xxx	-0.664	3.37

3.2.3. SEM Images of Corroded Coatings

The representative SEM micrographs taken from the surface of all coating layers after potentiodynamic polarisation tests in aerated 3.5% NaCl solution are shown in Figure 4. The state with which surfaces are relatively rough with microcracks could lead to WC-dissolution from the coating layers, which has been reported in refs [11, 18, 19]. Subsequently, the loss of the hard phase by dissolution of the binder during corrosion could set up galvanic corrosion between substrate and coating. For Figure 4c (brass coating), the surface layer remained relatively rough without falling off, although there were microcracks. This suggested that brass coatings had better bonding strength than stainless steel and super invar coatings, which could also have been responsible for the nobler OCP recorded. Figure 4a shows the SEM image of Aluminium 2xxx coating. The surface in the microstructure is nearly covered with protective oxide phase, Al_2O_3 . However, there were microcracks in the surface layer, and this could create active sites for galvanic corrosion, thereby affecting the corrosion resistance of aluminium 2xxx coating, as well as coated brass. In addition, the corroded surface of the coating were different despite same powder as feedstock. This could be due to the influence of the substrate properties on the coating (i.e. difference in coefficient of thermal expansion; differences in specific heat capacity; difference in melting point etc.).

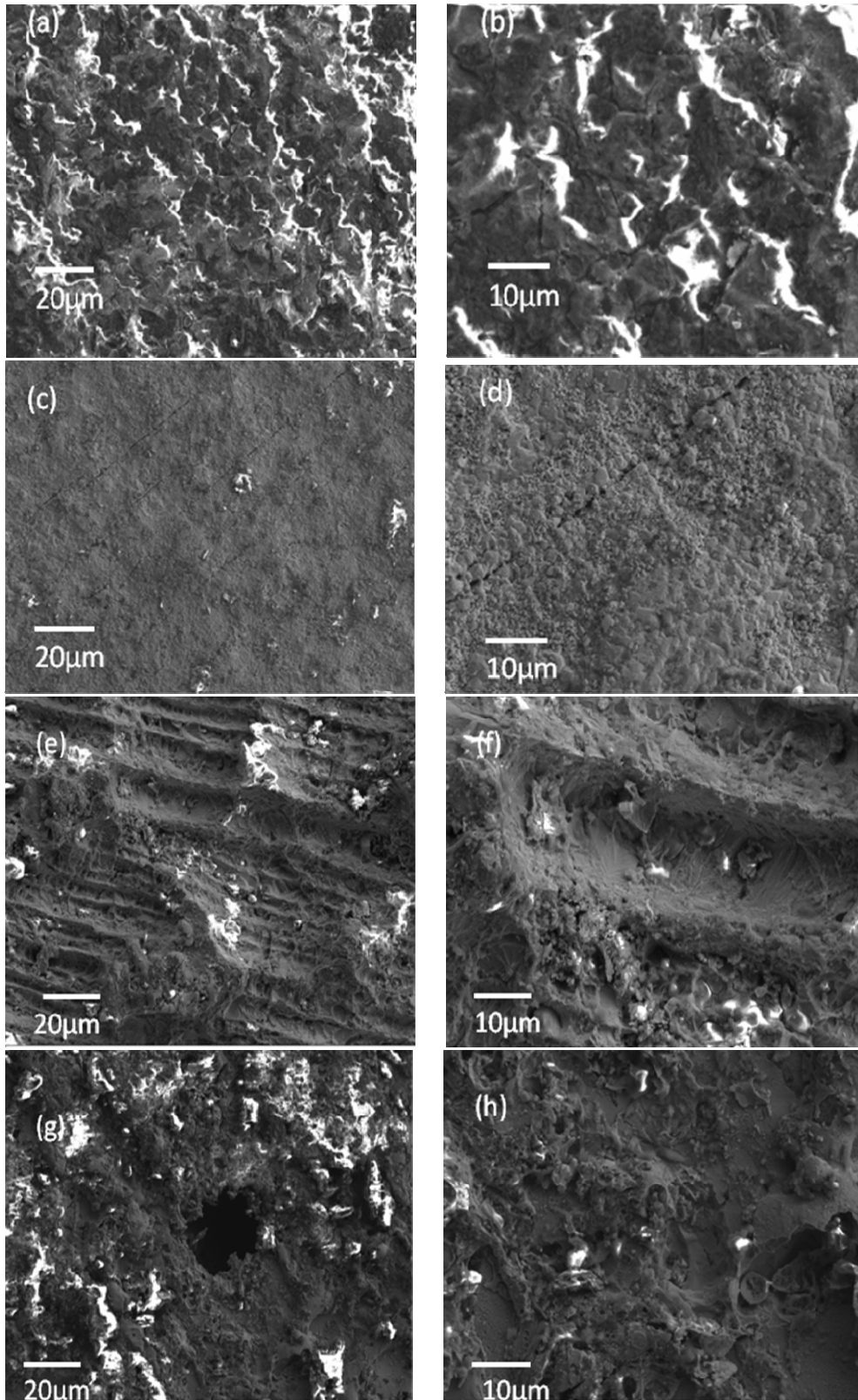


Figure 4. SEM/BSE micrographs of corrosion attack on the surface of (a, b) aluminium (c, d) Brass (e, f) Super-invar and (g, h) 304L stainless steel coated surfaces after immersion in 3.5% NaCl.

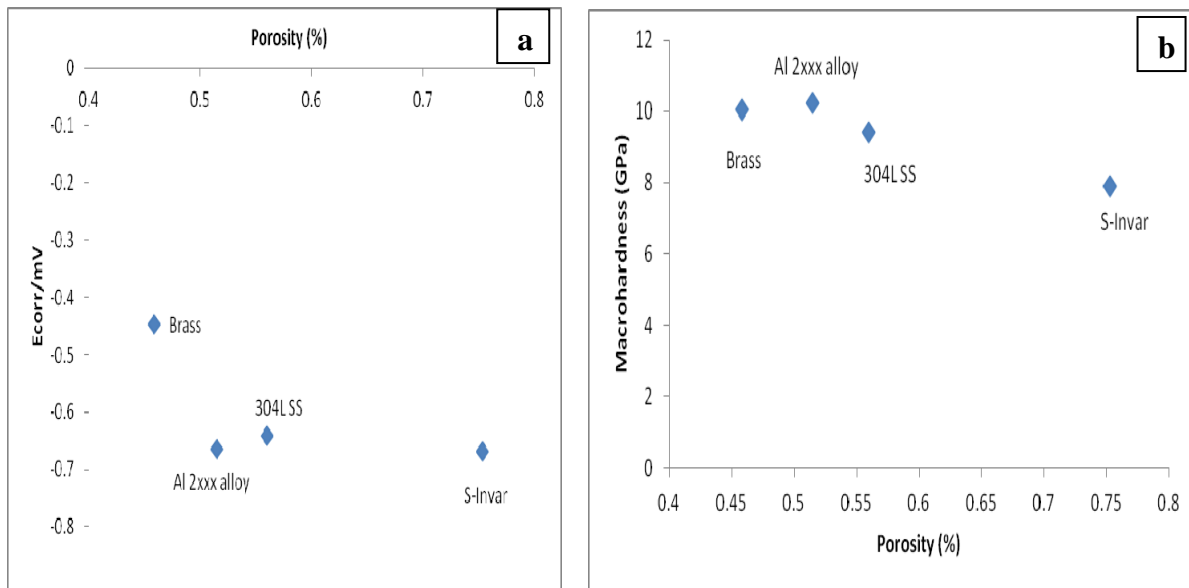


Figure 5: Correlation between (a) porosity and the corrosion rate, (b) porosity and the microhardness, of the WC-17Co coatings on the different substrate.

The relationships between the coating results as well as corrosion data are shown in Figure 5. The porosity was determined by dot counting techniques, (at high magnification). The corrosion rate decreased with increasing porosity (Figure 5a). Thus, strong correlations were observed between porosity and the corrosion rate as expected. The higher porosity sample had low E_{corr} , while low porosity sample indicated better E_{corr} (i.e. coated brass), showing that porosity was proportional to the corrosion rate. However, the little discrepancy of the as-coated aluminium 2xxx alloy might be attributed to the close porosity which was not determined during this work although the hardness decreased with an increasing in porosity. The corrosion rate does not show a discernable relationship with hardness. However, there are only four data points since the choice of substrate materials were based on their coefficient of their thermal expansion and industrial purpose. In addition, there was no relationship between the surface roughness and corrosion as the data was scatter. This is expected as corrosion deal with the degradation of material in an environment, while surface roughnesses only report the properties at the coated top bond alone.

Acknowledgement

The authors wish to acknowledge the financial and technical support of the Nuclear Energy Corporation of South Africa, the Department of Science and Technology, and National Research Foundation (South Africa).

Reference

A.K. Basak, P. Matteazzi, M. Vardavoulias, J.P. Celis, Corrosion-Wear Behaviour of Thermal Sprayed Nanostructured FeCu/WC-Co Coating, *Wear* 261 (2006) 1042-1050.

B. Vamsi Krishna, V.N. Misra, P.S. Mukherjee, P. Sharma, Microstructure and Properties of Flame Sprayed Tungsten Carbide Coatings, *International Journal of Refractory Metals and Hard Materials*, 20 (2012) 355-374.

B.Q. Wang, K. Luer, The Erosion – Oxidation Behaviour of HVOF Cr₃C₂ – NiCr Cermet Coating, *Wear* 174 (1994) 177-185.

D.E. Crawmer, Coating Structures, Properties, and Materials, *Handbook of Thermal Spray Technology*, J.R. Davis (Ed.), ASM International, 2005.

F. Vacandio, Y. Massiani, P. Gergaud, O. Thomas, Stress, Porosity Measurements and Corrosion Behaviour of AlN Films Deposited on Steel Substrates, *Thin Solid Films* 359 (2000) 221-227.

L.P. Ward, B. Hinton, D. Gerrard, and K. Short, Corrosion Behaviour of Modified HVOF Sprayed WC Based Cermet Coatings on Stainless Steel, *Journal of Minerals and Materials Characterization and Engineering* 10(11) (2006) 989-1005.

M. Takeda, T. Okabe, M. Kido and Y. Harada, Corrosion Behaviour of WC-Co and WC-Co-Cr Sprayed Coating in Na₂SO₄ Aqueous Solution, *Thermal Spray* 38 (2001) 58-64.

O.P. Oladijo, N. Sacks, L.A. Cornish and A.M. Venter, Effect of Substrate on the 3 Body Abrasion Wear of HVOF WC-17wt%Co Coatings, *International Journal of Refractory Metals and Hard Materials* 25 (2012) 288-294.

O.P. Oladijo, A.M. Venter, L.A. Cornish, Correlation between Residual Stress and Abrasive Wear of WC-17Co Coatings, International Journal of Refractory Metals and Hard Materials 44 (2014) 68-76.

P. Marcus, V. Maurice, Fundamental Aspects of Corrosion of Metallic Materials, Material Science and Engineering, 2 (1998) 1-34. <http://www.eolss.net/Eolss-sampleAllChapter.aspx>

U.T.C. Dragos, H. Losif, S. Viore-Aurel, F. Hannelore, Corrosion Properties of Cermet Coatings Sprayed by High Velocity Oxygen Fuel, Brno, Czech Republic, EU. Nanocon 10 (2012) 23-25.